

# Structured Channel Covariance Estimation from Limited Samples for Large Antenna Arrays

Tianyu Yang<sup>1</sup>, Mahdi Barzegar Khalilsarai<sup>1</sup>, Saeid Haghighatshoar<sup>2</sup>,  
and Giuseppe Caire<sup>1</sup>

## Abstract

In massive MIMO systems, the knowledge of channel covariance matrix is crucial for MMSE channel estimation in the uplink and plays an important role in several downlink multiuser beamforming schemes. Due to the large number of base station antennas in massive MIMO, accurate covariance estimation is challenging especially in the case where the number of samples is limited and thus comparable to the channel vector dimension. As a result, the standard sample covariance estimator yields high estimation error which may yield significant system performance degradation with respect to the ideal channel knowledge case. To address such covariance estimation problem, we propose a method based on a parametric representation of the channel angular scattering function. The proposed parametric representation includes a discrete specular component which is addressed using the well-known Multiple Signal Classification (MUSIC) method, and a diffuse scattering component, which is modeled as the superposition of suitable dictionary functions. To obtain the representation parameters we propose two methods, where the first solves a non-negative least-squares problem and the second maximizes the likelihood function using expectation-maximization. Our simulation results show that the proposed methods outperform the state of the art with respect to various estimation quality metrics and different sample sizes.

## Index Terms

Massive MIMO, covariance estimation, MUSIC, Maximum-Likelihood, Non-Negative Least Squares, Angular Scattering Function.

<sup>1</sup>Communications and Information Theory Group (CommIT), Technische Universität Berlin ({tianyu.yang, m.barzegarkhalilsarai, caire}@tu-berlin.de).

<sup>2</sup>Saeid Haghighatshoar is currently with the Swiss Center for Electronics and Microtechnology (CSEM), however his contribution to this work was made while he was with the CommIT group (saeid.haghighatshoar@csem.ch).

## I. INTRODUCTION

Massive Multiple-Input Multiple-Output (MIMO) communication system, where the number of base station (BS) antennas  $M$  is much larger than the number of single antenna users, has been shown to achieve high spectral efficiency in wireless cellular networks and enjoy various system level benefit, such as energy efficiency, inter-cell interference reduction, and dramatic simplification of user scheduling (e.g., see [1, 2]). In a large number of papers on the subject, the knowledge of the uplink (UL) and downlink (DL) channel covariance matrix, i.e., of the correlation structure of the channel antenna coefficients at the BS array, is assumed and used for a variety of purposes, such as MMSE UL channel estimation and pilot decontamination [3–5], efficient DL multiuser precoding/beamforming design, especially in the frequency division duplexing (FDD) case [6–10].

Under the usual assumption of wide-sense stationary (WSS) uncorrelated scattering (US), the channel vector evolves over time as a vector-valued WSS process and its spatial correlation is frequency-invariant over intervals much smaller than the carrier frequency. In particular, in an OFDM system, the channel spatial covariance is independent of time (OFDM symbol index) and frequency (subcarrier index). In order to capture the actual WSS statistics, samples sufficiently spaced over time and frequency must be collected (e.g., one sample for every resource block in the UL slots over which a given user is active). On the other hand, the WSS model holds only locally, over time intervals where the propagation geometry (angle and distances of multipath components) does not change significantly. Such time interval, often referred to as “geometry coherence time”, is several orders of magnitude larger than the coherence time of the small-scale channel coefficients. For a typical mobile urban environment, the channel geometry coherence time is of the order of seconds, while the small-scale fading coherence time is of the order of milliseconds (see [11] and references therein).<sup>1</sup> Hence, the BS can collect a window of tens-to-hundreds of noisy channel snapshots from UL pilot symbols sent by any given user, and use these samples to produce a “local” estimate of the corresponding user covariance matrix which remains valid during a channel geometry coherence time. Such estimation must be repeated, or updated, a rate that depends on the propagation scenario and user-BS relative motion. This

<sup>1</sup>See also [12] for a recent study based on data gathered from a channel sounder in an urban environment with a receiver moving at vehicular speed.

discussion points out that the number of samples  $N$  available for covariance estimation is limited and often comparable or even less than the number of BS antennas  $M$ . Therefore, the accurate estimation of the high-dimensional  $M \times M$  spatial channel covariance matrix (both in the UL and in the DL) from a limited number of noisy samples is generally a difficult task.

The simplest way to estimate the channel covariance matrices is the sample covariance estimator. Such estimation is asymptotically unbiased and consistent and works well when  $N \gg M$ . Unfortunately, as already noticed above, this is typically not the case in massive MIMO. Hence, the goal of this paper is to devise new parametric estimators that outperform the sample covariance estimator, as well as the other state-of-the-art methods proposed in the literature. In addition, an attractive feature of the proposed parametric estimation is that it lends itself to the extrapolation of the estimated channel covariance matrix from the UL to the DL frequency band. As the channel samples are collected by the BS through pilot symbols sent by the users on the UL, the UL channel covariance can be directly estimated via our method. However, as pointed out above, several schemes for DL multiuser precoding/beamforming in FDD systems make use of the user channel covariance matrix in the DL, which differs from the UL covariance since the frequency separation between the UL and the DL bands is large. The estimation of the DL covariance from UL channel samples has been considered in several works and it is generally another challenging task [6, 13–17]. We shall see that our scheme is able to accurately estimate the DL channel covariance by extrapolating (over frequency) the estimated parametric model in the UL.

#### *A. Related Work*

Covariance estimation from limited samples is a very well-known classical problem in statistics. In the “large system regime” when both the vector dimension  $M$  and the number of samples  $N$  grow large with fixed sampling ratio  $N/M$  of samples per dimension, a vast literature focused on the asymptotic eigenvalue distribution of sample covariance matrix estimator under specific statistical assumptions (see, e.g., [18–20] and the refs. therein). Covariance estimation has reemerged recently in many problems in machine learning, compressed sensing, biology, etc. (see, e.g., [21–24] from some recent results). What makes these recent works different from the classical ones is the highly-structured nature of the covariance matrices in these applications. A key challenge in these new applications is to design efficient estimation algorithms able to take

advantage of the underlying structure to recover the covariance matrix with a small sample size.

As we explain in the sequel, MIMO covariance matrices are also a class of highly-structured covariance matrices due to the particular spatial configuration of the BS antennas and wireless propagation scenario. So, it is very important to design efficient algorithms that are able to take advantage of this specific structure. In this paper, we shall compare our proposed method with alternative approaches which can be regarded as the state-of-the-art for the specific case of wireless massive MIMO channels. The competitor methods shall be briefly discussed when presenting such comparison results.

### B. Contributions

The main contributions of this work are listed below:

- In contrast to the previous works that either focused on diffuse scattering, such that the received power from any given angle direction is infinitesimal [13], or only on separable discrete components [25, 26], we propose a method that handles the more realistic mixed model where discrete and diffuse scattering is simultaneously present. This corresponds to a so-called “spiked model” in the language of asymptotic random matrix theory (e.g., see [20]), where the spikes are the discrete scattering components.
- The new idea of the proposed approach consists of a parametric model of the channel *angular scattering function* (ASF) in terms of atoms of a dictionary, formed by some Dirac delta functions placed at the angle-of-arrival (AoA) of the discrete specular components, and by a family of functions obtained by shifts of a template density function over the angle domain, in order to approximate the diffuse component of the ASF. We use Multiple Signal Classification (MUSIC) [27] to obtain the AoAs of the spikes (discrete scattering components).
- After having the estimated AoAs of the spikes via MUSIC, we propose two estimators, namely a constrained Least-Square estimator and Maximum-Likelihood (ML) estimator, to obtain the parametric model coefficients. In particular, the maximization of the likelihood function in the ML estimator is obtained via the expectation maximization (EM) initialized by the constrained Least-Squares solution.
- We present several numerical results with comparison with other competitor schemes. Our comparison shows that the proposed algorithms outperform the competitor schemes over

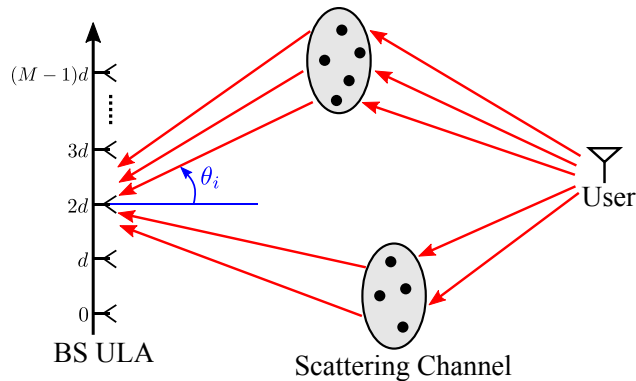


Fig. 1: A cartoonish representation of a multipath propagation channel, where the user signal is received at the BS through two scattering clusters.

all benchmarks in a wide range of sampling ratio  $N/M$ .

### C. Used Notations

An identity matrix with  $K$  columns is denoted as  $\mathbf{I}_K$ . An all-zero matrix with size  $m \times n$  is denoted as  $\mathbf{0}_{m \times n}$ .  $\text{diag}(\cdot)$  returns a diagonal matrix.  $\|\cdot\|_F$  returns Frobenius norm of a matrix.  $\delta(\cdot)$  denotes Dirac delta function. We use  $[n]$  to denote the ordered integer set  $\{1, 2, \dots, n\}$ .

## II. SYSTEM MODEL

We consider a typical single-cell massive MIMO communication system, where a BS equipped with a uniform linear array (ULA) of  $M$  antennas communicates with multiple users through a scattering channel.<sup>2</sup> Fig. 1 visualizes the propagation model based on multipath clusters, which is physically motivated and widely adopted in standard channel simulation tools such as QuaDriGa [28]. During UL transmission, on each time-frequency resource block (RB)  $s$  the BS receives an UL user pilot carrying a measurement for the channel vector  $\mathbf{h}(s)$ . We assume that the window of  $N$  samples collected for covariance estimation is designed such that the samples are enough spaced in the time-frequency domain such that the channel snapshots  $\{\mathbf{h}(s) : s = [N]\}$  are statistically independent, but the whole window spans a time significantly shorter than the geometry coherence time, such that the WSS assumption holds (see discussion in Section I) and

<sup>2</sup>Notice that in the case of a multi-cell system with pilot contamination the same techniques of this paper can estimate the covariance of the sum of multiple channels, and a pilot decontamination scheme as described in [9] can be applied. However, this goes beyond the scope of this paper.

the channel snapshots are identically distributed. The channel vectors are given by

$$\mathbf{h}[s] = \int_{-1}^1 \rho(\xi; s) \mathbf{a}(\xi) d\xi, \quad s \in [N], \quad (1)$$

where  $\rho(\xi; s)$  is the random channel gain over the normalized AoA  $\xi = \frac{\sin(\theta)}{\sin(\theta_{\max})} \in [-1, 1)$ , where  $\theta_{\max} \in [0, \frac{\pi}{2}]$  is the maximum array angular aperture.  $\mathbf{a}(\xi) \in \mathbb{C}^M$  denotes the array response vector at  $M$  BS antennas over  $\xi$ , whose  $m$ -th element is given as  $[\mathbf{a}(\xi)]_m = e^{j\frac{2\pi d}{\lambda_0} m \xi \sin(\theta_{\max})}$ , where  $d$  denotes the antenna spacing and  $\lambda_0$  denotes the carrier wavelength. For convenience we assume the antenna spacing to be  $d = \frac{\lambda_0}{2 \sin(\theta_{\max})}$ . Thus, the array response vector is given as

$$\mathbf{a}(\xi) = [1, e^{j\pi\xi}, \dots, e^{j\pi(M-1)\xi}]^T. \quad (2)$$

The channel gain  $\rho(\xi; s)$  is to be a complex Gaussian process with zero mean and autocorrelation function

$$\mathbb{E}[\rho(\xi; s) \rho^*(\xi'; s)] = \gamma(\xi) \delta(\xi - \xi'), \quad (3)$$

where  $\gamma : [-1, 1] \rightarrow \mathbb{R}_+$  is a real non-negative measure that describes how the channel energy is distributed across the angle domain. We refer to  $\gamma(\xi)$  as the channel ASF. Notice that (3) is time-invariant (independent of  $s$ ) and uncorrelated with respect to  $\xi$ , consistently with the WSS-US assumption. The channel covariance matrix is given by

$$\Sigma_{\mathbf{h}} = \mathbb{E}[\mathbf{h}[s]\mathbf{h}[s]^H] = \int_{-1}^1 \gamma(\xi) \mathbf{a}(\xi) \mathbf{a}(\xi)^H d\xi. \quad (4)$$

At RB  $s$ , the received pilot signal at the BS is given as

$$\mathbf{y}[s] = \mathbf{h}[s]x[s] + \mathbf{z}[s], \quad s \in [N], \quad (5)$$

where  $x[s]$  is the pilot symbol and  $\mathbf{z}[n] \sim \mathcal{CN}(\mathbf{0}, N_0 \mathbf{I})$  is the additive white Gaussian noise (AWGN). Without loss of generality, we assume that the pilot symbols are normalized as  $x[n] = 1, \forall s \in [N]$ . The goal of this work is to estimate the channel covariance matrix  $\Sigma_{\mathbf{h}}$  with the given set of  $N$  noisy channel observations  $\{\mathbf{y}[s] : s \in [N]\}$ .

#### A. Sample Covariance Matrix Estimation

We start by reviewing the sample covariance estimator. For known noise variance  $N_0$  be known at the BS, the sample covariance matrix is given by:

$$\widehat{\Sigma}_{\mathbf{h}} = \frac{1}{N} \sum_{s=1}^N \mathbf{y}[s]\mathbf{y}[s]^H - N_0 \mathbf{I}. \quad (6)$$

This is a consistent estimator, in the sense that it converges to the true covariance matrix as  $N \rightarrow \infty$  [29]. The mean square (Frobenius-norm) error incurred by the sample covariance estimator

is given as [29]  $\mathbb{E} \left[ \left\| \widehat{\Sigma}_{\mathbf{h}} - \Sigma_{\mathbf{h}} \right\|_{\text{F}}^2 \right] = \frac{\text{tr}(\Sigma_{\mathbf{h}})^2}{N}$ . By applying the Cauchy-Schwarz inequality to the singular values of  $\Sigma_{\mathbf{h}}$ , it is seen that  $\text{tr}(\Sigma_{\mathbf{h}}) \leq \|\Sigma_{\mathbf{h}}\|_{\text{F}} \sqrt{\text{rank}(\Sigma_{\mathbf{h}})}$ , which together with the estimation error expression yields the upper bound to the normalized mean squared error

$$\mathbb{E} \left[ \frac{\left\| \widehat{\Sigma}_{\mathbf{h}} - \Sigma_{\mathbf{h}} \right\|_{\text{F}}^2}{\|\Sigma_{\mathbf{h}}\|_{\text{F}}^2} \right] \leq \frac{\text{rank}(\Sigma_{\mathbf{h}})}{N}. \quad (7)$$

As already discussed, a relevant and interesting regime for massive MIMO is when  $N/M \approx 1$ . From the above analysis, it is clear that the sample covariance estimator yields a small error if  $\text{rank}(\Sigma_{\mathbf{h}}) \ll N$ . For example, if the scattering contains only a finite number of discrete components (e.g., the line-of-sight propagation and a few specular reflections)  $\text{rank}(\Sigma_{\mathbf{h}})$  is finite even if  $M$  is very large. In contrast, if  $\gamma(\xi)$  contains a diffuse scattering component, i.e., if its cumulative distribution function  $\Gamma(\xi) = \int_{-1}^{\xi} \gamma(\nu) d\nu$  is piecewise continuous with strictly monotonically increasing segments, then  $\text{rank}(\Sigma_{\mathbf{h}})$  increases linearly with  $M$  (see [10]) and the error incurred by the sample covariance estimator can be large. On the other hand, the presence of discrete scattering components implies that  $\gamma(\xi)$  contains Dirac delta functions (spikes) and therefore it is not squared-integrable. This poses significant problems for estimation methods that assume  $\gamma(\xi)$  to be an element in a Hilbert space of functions (e.g., the method proposed in [13]). The challenge tackled in this work is to handle both the small sample regime  $N/M \leq 1$  and the presence of both discrete and diffuse scattering.

### B. Structure of the channel covariance matrix

We assume that the ASF  $\gamma(\xi)$  can be decomposed into its discrete and diffuse scattering components as

$$\gamma(\xi) = \gamma_d(\xi) + \gamma_c(\xi) = \sum_{i=1}^r c_i \delta(\xi - \xi_i) + \gamma_c(\xi), \quad (8)$$

where  $\gamma_d(\xi)$  models the power received from  $r \ll M$  discrete paths and  $\gamma_c(\xi)$  models the power coming from diffuse scattering clusters. Since the ASF can be seen as a (generalized) density function, we borrow the language of discrete and continuous random variables and refer to  $\gamma_d(\xi)$  and to  $\gamma_c(\xi)$  as the *discrete* and the *continuous* parts of the ASF, respectively.<sup>3</sup> We also assume that  $\text{supp}(\gamma) = \Xi$  has a Lebesgue measure significantly less than 2, i.e., the continuous part of

<sup>3</sup>As for probability density functions,  $\gamma_c(\xi)$  needs not be continuous, but its cumulative distribution function  $\Gamma_c(\xi) = \int_{-1}^{\xi} \gamma_c(\nu) d\nu$  is a continuous function.

the ASF  $\gamma_c(\xi)$  has a limited angular support, due to the localized geometry of the scattering clusters (e.g., see [28]).

Plugging (8) into (4) we obtain a corresponding decomposition of the channel covariance matrix as

$$\Sigma_{\mathbf{h}} = \Sigma_{\mathbf{h}}^d + \Sigma_{\mathbf{h}}^c = \sum_{i=1}^r c_i \mathbf{a}(\xi_i) \mathbf{a}(\xi_i)^H + \int_{-1}^1 \gamma_c(\xi) \mathbf{a}(\xi) \mathbf{a}(\xi)^H d\xi, \quad (9)$$

where  $\Sigma_{\mathbf{h}}^d$  is a rank- $r$ , positive semi-definite (PSD) matrix.

In order to model the continuous part of the ASF, we notice that in typical channel models  $\gamma_c(\xi)$  consists of several support-disjoint subcomponents, i.e.,  $\gamma_c(\xi) = \sum_{k=1}^{r'} \gamma_c^{(k)}(\xi)$ , where each  $\gamma_c^{(k)}$  corresponds to a diffuse scattering cluster with given center angle and angular spread  $\text{supp}(\gamma_c^{(k)}) = \Xi_k \subset \Xi$ . For given typical propagation environments, the support size of clusters satisfies  $|\Xi_k| \leq S_{\max}$  for some environment-specific upper bound  $S_{\max}$ . Hence, the intuition underlying our approach is that  $\gamma_c^{(k)}(\xi)$  can be well approximated by the sparse (or block-sparse) superposition of “template” support-limited non-negative dictionary functions. The choice of the dictionary functions can be made according to some educated guess about the typical shape of the scattering clusters (more discussion and examples will be provided in the following).

### III. DICTIONARY-BASED PARAMETRIC REPRESENTATION AND COVARIANCE ESTIMATION

An outline of the steps taken by our proposed method is given in the following:

i) *Spike Location Estimation for  $\gamma_d(\xi)$* : We apply the MUSIC algorithm [27] to estimate the AoAs of the spike components, i.e., the angles  $\{\xi_i\}_{i=1}^r$  in (8), from the  $N$  noisy samples  $\{\mathbf{y}[s] : s \in [N]\}$ . We let  $\{\hat{\xi}_i\}_{i=1}^{\hat{r}}$  denote the estimated AoAs, where also the number of spikes  $\hat{r}$  is estimated (not assumed known). This is detailed in Section IV. It can be shown that for a finite number of spikes  $r$ , as the number of antennas  $M$  and the number of samples  $N$  grow to infinity with fixed ratio, MUSIC yields an asymptotically consistent estimate of the spike AoAs, please refer to the proof in our previous paper [30, Theorem 1]. For complete estimation of the discrete part  $\Sigma_{\mathbf{h}}^d$ , the weights  $\{c_i\}_{i=1}^{\hat{r}}$  need to be further recovered. This is done jointly with the coefficients of the continuous part, as elaborated in the next step.

ii) *Dictionary-based Method for Joint Estimation of  $\gamma_d(\xi)$  and  $\gamma_c(\xi)$* : We assume that the ASF continuous part can be written as

$$\gamma_c(\xi) = \sum_{i=1}^G b_i \psi_i(\xi), \quad (10)$$



where  $\mathcal{G}_c = \{\psi_i(\xi) : i \in [G]\}$  is a suitable dictionary of non-negative density functions (not containing spikes). Now the goal is to estimate the model parameters  $\{c_i\}_{i=1}^{\widehat{r}}$  and  $\{b_i\}_{i=1}^G$  assuming the form of ASF  $\gamma(\xi) = \sum_{i=1}^{\widehat{r}} c_i \delta(\xi - \widehat{\xi}_i) + \sum_{i=1}^G b_i \psi_i(\xi)$ . The parameters estimation can be formulated as a constrained Least-Squares problem, as detailed in Section V. In particular, if the functions in  $\mathcal{G}_c$  have disjoint support, we obtain a Non-negative Least-Squares (NNLS) problem while if the functions in  $\mathcal{G}_c$  have overlapping supports, we obtain a Quadratic Programming (QP) problem. As an alternative, we can use Maximum-Likelihood estimation. The log-likelihood function is difference of concave functions in the model parameters, and can be maximized using Maximization-Minimization (MM) methods. However, general MM approaches are prohibitively computationally complex for typical values of  $M$  arising in massive MIMO. It turns out that when  $\mathcal{G}_c$  is also formed by Dirac deltas spaced on a discrete grid, the likelihood function maximization can be obtained through Expectation Maximization (EM), with much lower complexity. Since in general both MM and EM are guaranteed to converge to local maxima, the initialization plays an important role. We propose to use the result of the (low-complexity) NNLS estimator as initial point for the EM iteration. The resulting method is detailed in Section VI.

iii) *From ASF to Covariance Estimation*: Finally, having estimated  $\gamma_d(\xi)$  and  $\gamma_c(\xi)$ , we estimate the covariance  $\Sigma_{\mathbf{h}}$  via (9). In particular, since  $\gamma(\xi)$  depends only on the scattering geometry and it is invariant with frequency,<sup>4</sup> the mapping  $\gamma(\xi) \rightarrow \Sigma_{\mathbf{h}}$  defined by (9) can be applied different carrier frequencies by changing the wavelength parameter  $\lambda_0$  in the expression of the array response vector  $\mathbf{a}(\xi)$ . Specifically, replacing  $\mathbf{a}(\xi)$  in (9) with  $\mathbf{a}(\nu\xi)$  where  $\nu$  is a wavelength expansion/contraction coefficient, we obtain an estimator at the carrier frequency  $f_\nu = \nu f_0$ , where  $f_0 = c_0/\lambda_0$  is the UL carrier frequency and  $c_0$  denotes the speed of light. The resulting covariance estimator is given by

$$\widehat{\Sigma}_{\mathbf{h}}^{(\nu)} = \sum_{i=1}^{G+\widehat{r}} u_i^* \mathbf{S}_i^{(\nu)}, \quad (11)$$

where  $\{u_i^* : i \in [G + \widehat{r}]\}$  are the estimated model parameters, and where we define  $\mathbf{S}_i^{(\nu)} = \int_{-1}^1 \psi_i(\xi) \mathbf{a}(\nu\xi) \mathbf{a}^H(\nu\xi) d\xi$  for  $i \in [G]$  and  $\mathbf{S}_{G+i}^{(\nu)} = \mathbf{a}(\nu\widehat{\xi}_i) \mathbf{a}^H(\nu\widehat{\xi}_i)$  for  $i = 1, \dots, \widehat{r}$ . In particular,

<sup>4</sup>This statement holds over not too large frequency ranges, where the scattering properties of materials is virtually frequency independent. For example, this property holds for the UL and DL carrier frequencies of the same FDD system, however it does not generally hold over much larger frequency ranges. For example, the ASFs of the same environment at (say) 3.5 GHz and at 28 GHz are definitely different, although quite related [31].

for the DL carrier we have  $\nu > 1$  since in typical cellular systems the DL carrier frequency is higher than the UL carrier frequency.

#### IV. DISCRETE ASF SUPPORT ESTIMATION

In this part, we use the MUSIC method [32] to estimate the number  $r$  as well as the support  $\{\xi_i\}_{i=1}^r$  of the spikes in the discrete part of the ASF  $\gamma_d(\xi)$ . MUSIC was originally proposed for estimating the number and also the frequency of several sinusoids from their mixture contaminated with noise (see, e.g., [33] and many references therein). Let

$$\hat{\Sigma}_{\mathbf{y}} = \frac{1}{N} \sum_{s=1}^N \mathbf{y}[s] \mathbf{y}[s]^H \quad (12)$$

be the sample covariance of the observation  $\{\mathbf{y}[s] : s \in [N]\}$ . Let  $\hat{\Sigma}_{\mathbf{y}} = \hat{\mathbf{U}} \hat{\Lambda} \hat{\mathbf{U}}^H$  be the eigendecomposition of  $\hat{\Sigma}_{\mathbf{y}}$ , where  $\hat{\Lambda} = \text{diag}(\hat{\lambda}_{1,M}, \dots, \hat{\lambda}_{M,M})$  denotes the diagonal matrix consisting of the eigenvalues of  $\hat{\Sigma}_{\mathbf{y}}$ . Without loss of generality, we assume that the eigenvalues are ordered as  $\hat{\lambda}_{1,M} \geq \dots \geq \hat{\lambda}_{M,M}$ . First, we wish to estimate the model order  $r$ . Intuitively, we expect to find  $r$  “large” eigenvalues containing the contribution of the spikes and  $M - r$  small eigenvalues containing only the contribution of the diffuse scattering and the noise. This jump between large and small eigenvalues of the sample covariance  $\hat{\Sigma}_{\mathbf{y}}$  becomes more and more evident as the number of antennas  $M$  becomes large. This can be explained by noticing that, as the array angular resolution increases, the amount of received signal energy in each angular bin decreases as the bin size if the ASF contains no delta functions in the bin, while it remains roughly constant with  $M$  if the angular bin contains a spike. More precisely, an angular bin of width  $2/M$  and centered at  $\xi$  contains a received signal power proportional to  $2(\gamma_c(\xi) + N_0)/M$  if no spike falls in the interval, and to  $c_i + 2(\gamma_c(\xi) + N_0)/M$  if the spike located at  $\xi_i$  falls in the interval. By Szegő’s theorem (e.g., see [10] and references therein), the eigenvalues of the covariance matrix  $\Sigma_{\mathbf{y}} = \Sigma_{\mathbf{h}} + N_0 \mathbf{I}_M$  converge asymptotically as  $M \rightarrow \infty$  to the energy received on equally spaced angular bins of width  $2/M$  over the interval  $[-1, 1]$  in the  $\xi$  domain. Hence, we expect that for large  $M$  the “jump” between large (constant with  $M$ ) and small (decreasing as  $1/M$ ) eigenvalues can be easily identified.<sup>5</sup> Fig. 2 corroborates our intuition showing the separation between the eigenvalues of the sample covariance matrix  $\hat{\Sigma}_{\mathbf{y}}$  for different number of

<sup>5</sup>This consideration is precisely supported by the study of spiked models in asymptotic random matrix theory [34], where it is proved that separation between the spikes and the “bulk” of the eigenvalues become wider and wider as  $M \rightarrow \infty$ .

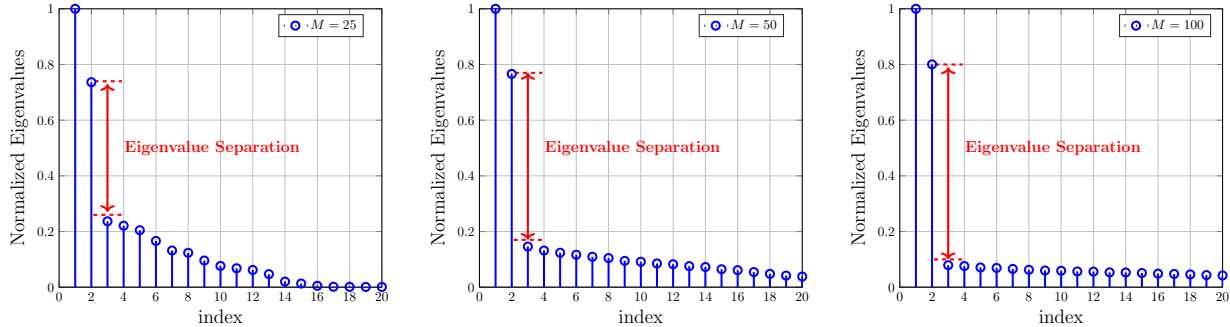


Fig. 2: Eigenvalue distribution for the sample covariance matrix  $\hat{\Sigma}_y(M)$  associated with the example ASF in (13) for different values of  $M$  and  $N/M = 2$ .

antennas  $M = 25, 50, 100$  with fixed sample size to channel dimension ratio  $N/M = 2$  and the same channel geometry defined by the ASF

$$\gamma(\xi) = \text{rect}_{[-0.7, -0.4]} + \text{rect}_{[0, 0.6]} + (\delta(\xi + 0.2) + \delta(\xi - 0.4))/2, \quad (13)$$

where  $\text{rect}_{\mathcal{A}}$  is 1 over the interval  $\mathcal{A}$  and zero elsewhere. This ASF contains  $r = 2$  spikes and two rectangular-shaped diffuse components. The SNR is set to 20 dB. For a large enough number of antennas (and even for a moderate number such as  $M = 25$ ) the eigenvalue distribution shows a significant jump, such that the two largest eigenvalues “escape” from the rest. Note that, by increasing the number of antennas, this separation becomes more and more significant. From the above intuition, we propose the following method based on  $K$ -means clustering. **Estimating the Number of Spikes  $r$  via  $K$ -means.** We first normalize the eigenvalues by the largest eigenvalue  $\hat{\lambda}_{1,M}$  and define the normalized parameters  $\beta_i = \left(\frac{\hat{\lambda}_{i,M}}{\hat{\lambda}_{1,M}}\right)^p$ , where  $p \in (0, 1)$  and  $\beta_i \in [0, 1] \forall i \in [M]$ . The role of the exponent  $p \in (0, 1)$  is to soft-truncate the larger eigenvalues. This can be simply seen by considering the function  $f : x \mapsto x^p$  in the interval  $x \in [0, 1]$ , where for  $p \in (0, 1)$  the function  $f$  is quite flat around  $x_0 = 1$ . In this way, all the  $x$ -values in a large neighborhood of  $x_0 = 1$  are mapped to a very small neighborhood of  $f(x_0) = f(1) = 1$ . Thus, the larger eigenvalues correspond to values  $\beta_i$  that accumulate close to 1 (soft-truncated). In our simulations we use  $p = \frac{1}{2}$ , which was empirically determined to yield good results for the considered system parameters.

After the normalization of the eigenvalues, we run the  $K$ -means clustering algorithm with  $K = 2$  clusters over the 1-dim set of normalized parameters  $\{\beta_i : i \in [M]\}$ , where we initialize the centers of the two clusters with values chosen uniformly and randomly in the interval  $[0, 1]$ .

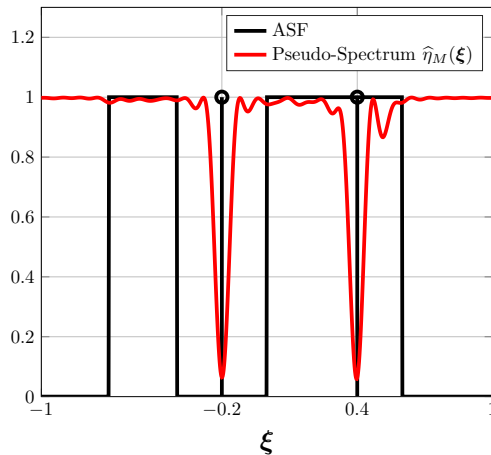


Fig. 3: The pseudo-spectrum plotted for the example ASF in (13) with  $M = 25$  and  $N/M = 2$ .

Denoting by  $c_{\max}^{(\infty)}$  and  $c_{\min}^{(\infty)}$  the final centers of the clusters after the convergence of the  $K$ -means algorithm and assuming without loss of generality that  $c_{\min}^{(\infty)} \leq c_{\max}^{(\infty)}$ , we approximate the number of spikes  $\hat{r}$  by the number of points  $\beta_i$  falling in the cluster centered at  $c_{\max}^{(\infty)}$ .

Of course, this method may recover *fake* spikes by overestimating the true  $r$  (especially when  $p$  is close to 0 such that the larger singular values are too much soft-truncated). However, we shall see later that overcounting the spikes is not a big problem in the overall covariance estimation scheme, since the coefficients of fake spikes are typically estimated as close to zero in the model coefficient estimation step described in the next two sections. In other words, it is always better to overestimate the number of spikes than to underestimate them so that the true spikes are not missed. This suggests also to pick a soft-truncation exponent  $p$  not too small.

Once the number of spikes is estimated as described above, MUSIC proceeds to identify the locations of those spikes. Let  $\hat{\mathbf{u}}_{\hat{r}+1,M}, \dots, \hat{\mathbf{u}}_{M,M}$  be the eigen-vectors in  $\hat{\mathbf{U}}$  corresponding to the smallest  $M - \hat{r}$  eigenvalues and let us define  $\mathbf{U}_{\text{noi}} = [\hat{\mathbf{u}}_{\hat{r}+1,M}, \dots, \hat{\mathbf{u}}_{M,M}]$  as the  $M \times (M - \hat{r})$  matrix corresponding to the noise subspace. The MUSIC objective function is defined as the pseudo-spectrum:

$$\hat{\eta}_M(\xi) = \|\mathbf{U}_{\text{noi}}^H \mathbf{a}(\xi)\|^2 = \sum_{k=\hat{r}+1}^M |\mathbf{a}(\xi)^H \hat{\mathbf{u}}_{k,M}|^2. \quad (14)$$

MUSIC estimates the support  $\{\hat{\xi}_1, \dots, \hat{\xi}_{\hat{r}}\}$  of the spikes by identifying  $\hat{r}$  dominant minimizers of  $\hat{\eta}_M(\xi)$ . Fig 3 illustrates the normalized values of the pseudo-spectrum (14) for the example ASF in (13) and its corresponding sample covariance  $\hat{\Sigma}_y$  for  $M = 25$  and  $N/M = 2$ . As we can

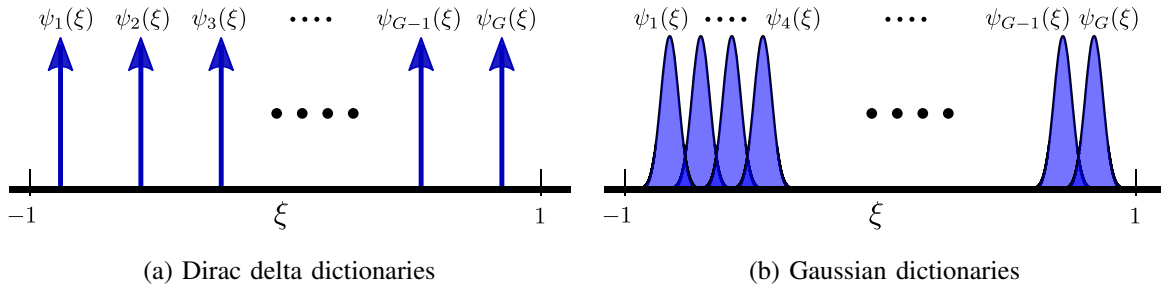


Fig. 4: Examples of Dirac delta and Gaussian dictionaries

see, the  $r = 2$  smallest minima of the pseudo-spectrum occur very close to the points  $\xi = -0.2$  and  $\xi = 0.4$ , which are the locations of the spikes in the true ASF.

## V. COEFFICIENTS ESTIMATION BY CONSTRAINED LEAST-SQUARES

Up to this point we have an estimate of the spike locations as  $\{\widehat{\xi}_i\}_{i=1}^{\widehat{r}}$  and therefore of the discrete ASF component in the form  $\widehat{\gamma}_d(\xi) = \sum_{i=1}^{\widehat{r}} c_i \delta(\xi - \widehat{\xi}_i)$ , where the non-negative coefficients vector  $\mathbf{c} = [c_1, \dots, c_{\widehat{r}}]^T \in \mathbb{R}_+^{\widehat{r}}$  is yet to be estimated. As said before, we consider an approximation of the continuous ASF component  $\gamma_c(\xi)$  in the form (10), where  $\mathbf{b} = [b_1, \dots, b_G]^T \in \mathbb{R}^G$  denotes the real-valued vector of coefficients. This assumption greatly simplifies the estimation task and transforms it from estimating an infinite-dim function  $\gamma_c(\xi)$  to estimate a finite-dimensional real vector  $\mathbf{b}$ . The dictionary functions  $\{\psi_i(\xi)\}$  are selected according to the available prior knowledge about the propagation environment. Some typical choices include localized functions  $\psi_i(\xi)$ , such as Gaussian, Laplacian, or rectangular functions, with a suitably chosen support. Fig. 4 shows an example of Dirac delta and Gaussian dictionaries.

The above representation of the ASF results in the parametric form of the channel covariance given by

$$\boldsymbol{\Sigma}_h(\mathbf{u}) = \sum_{i=1}^{G+\widehat{r}} u_i \mathbf{S}_i, \quad (15)$$

where we define the model parameter vector  $\mathbf{u} = [u_1, \dots, u_{G+\widehat{r}}]^T = [b_1, \dots, b_G, c_1, \dots, c_{\widehat{r}}]^T$  and the positive semi-definite matrices  $\mathbf{S}_i = \int_{-1}^1 \psi_i(\xi) \mathbf{a}(\xi) \mathbf{a}(\xi)^H d\xi$  for  $i \in [G]$ , and  $\mathbf{S}_{i+G} = \mathbf{a}(\widehat{\xi}_i) \mathbf{a}(\widehat{\xi}_i)^H$  for  $i \in [\widehat{r}]$ .

In order to estimate the coefficients vector  $\mathbf{u}$  from the noisy samples  $\{\mathbf{y}[s] : s \in [N]\}$ , we propose three algorithms, namely the NNLS estimator, QP estimator and the ML-EM estimator.

### A. NNLS estimator

If the dictionary functions have disjoint support, since the overall  $\gamma_c(\xi)$  must be non-negative, it follows that the coefficients  $\{u_i : i = [G]\}$  must take values in  $\mathbb{R}_+$ , i.e., the whole vector  $\mathbf{u}$  is non-negative. We know that if the number of samples  $N$  is large enough, the sample covariance matrix  $\widehat{\Sigma}_y$  would converge to  $\Sigma_y = \Sigma_h + N_0\mathbf{I}$ . Then, our goal is to find a good fitting to the sample covariance matrix  $\widehat{\Sigma}_y$  from the set of all covariance matrices of the form

$$\Sigma_y = \Sigma_h(\mathbf{u}) + N_0\mathbf{I} = \sum_{i=1}^{G+\widehat{r}} u_i \mathbf{S}_i + N_0\mathbf{I}. \quad (16)$$

For this purpose, we use the Frobenius norm as a fitting metric and obtain an estimate of the model coefficients as

$$\mathbf{u}^* = \arg \min_{\mathbf{u} \in \mathbb{R}_+^{G+\widehat{r}}} \left\| \widehat{\Sigma}_y - \sum_{i=1}^{G+\widehat{r}} u_i \mathbf{S}_i - N_0\mathbf{I} \right\|_F^2, \quad (17)$$

$$= \arg \min_{\mathbf{u} \in \mathbb{R}_+^{G+\widehat{r}}} \left\| \widehat{\Sigma}_h - \sum_{i=1}^{G+\widehat{r}} u_i \mathbf{S}_i \right\|_F^2. \quad (18)$$

Applying vectorization and defining  $\mathbf{A} = [\text{vec}(\mathbf{S}_1) \dots \text{vec}(\mathbf{S}_{G+\widehat{r}})]$  and  $\mathbf{f} = \text{vec}(\widehat{\Sigma}_h)$ , we can write this as a NNLS problem

$$\mathbf{u}^* = \arg \min_{\mathbf{u} \in \mathbb{R}_+^{G+\widehat{r}}} \|\mathbf{A}\mathbf{u} - \mathbf{f}\|^2, \quad (19)$$

which can be efficiently solved using a variety of convex optimization techniques (see, e.g., [35, 36]). In our simulation, we use the built-in MATLAB function *lsqnonneg*.

Note that a ULA covariance is Hermitian Toeplitz. By leveraging this, we can reformulate the optimization problem so that the problem dimension is reduced. Concretely, let  $\widetilde{\Sigma}_h$  denote the orthogonal projection of  $\widehat{\Sigma}_h$  onto the space of Hermitian Toeplitz matrices. This is obtained by averaging the diagonals of  $\widehat{\Sigma}_h$  and replacing the diagonal elements by the corresponding average value (see Appendix for completeness). We define the first column of  $\widetilde{\Sigma}_h$  as  $\widetilde{\boldsymbol{\sigma}}$ . Then, (19) can be reformulated as

$$\mathbf{u}^* = \arg \min_{\mathbf{u} \in \mathbb{R}_+^{G+\widehat{r}}} \left\| \mathbf{W} \left( \widetilde{\mathbf{A}}\mathbf{u} - \widetilde{\boldsymbol{\sigma}} \right) \right\|^2, \quad (20)$$

where  $\widetilde{\mathbf{A}} = [(\mathbf{S}_1)_{\cdot,1}, \dots, (\mathbf{S}_{G+\widehat{r}})_{\cdot,1}]$  is the matrix collecting the first columns  $(\mathbf{S}_i)_{\cdot,1}$  of the  $\mathbf{S}_i$  and  $\mathbf{W} = \text{diag} \left( \left[ \sqrt{M}, \sqrt{2(M-1)}, \sqrt{2(M-2)}, \dots, \sqrt{2} \right]^T \right)$  is the weighting matrix to compensate for the number of times an element is repeated in a Hermitian Toeplitz matrix.

**Lemma 1:** The optimization problems in (19) and (20) are equivalent.

*Proof:* Note that the difference between (19) and (20) is only the replacement of  $\tilde{\Sigma}_{\mathbf{h}}$  from  $\hat{\Sigma}_{\mathbf{h}}$ . Thus, it is sufficient to show the equivalence of the following two optimization problems:

$$\text{P1: } \min_{\mathbf{X} \in \mathcal{HT}} \|\mathbf{X} - \hat{\Sigma}_{\mathbf{h}}\|_{\text{F}}^2, \quad \text{P2: } \min_{\mathbf{X} \in \mathcal{HT}} \|\mathbf{X} - \tilde{\Sigma}_{\mathbf{h}}\|_{\text{F}}^2, \quad (21)$$

where  $\mathcal{HT}$  is the set of Hermitian Toeplitz matrices. Let  $\Delta = \hat{\Sigma}_{\mathbf{h}} - \tilde{\Sigma}_{\mathbf{h}}$ . Then, P1 is rewritten as  $\min_{\mathbf{X} \in \mathcal{HT}} \|\mathbf{X} - \tilde{\Sigma}_{\mathbf{h}} - \Delta\|_{\text{F}}^2$ . Since  $\tilde{\Sigma}_{\mathbf{h}}$  is the orthogonal projection of  $\hat{\Sigma}_{\mathbf{h}}$  on the set  $\mathcal{HT}$ , by the orthogonality principle the difference  $\Delta = \hat{\Sigma}_{\mathbf{h}} - \tilde{\Sigma}_{\mathbf{h}}$  is orthogonal to the whole set, i.e.,  $\langle \Delta, \mathbf{T} \rangle := \text{tr}(\Delta^{\text{H}}\mathbf{T}) = 0, \forall \mathbf{T} \in \mathcal{HT}$ . It follows that for any  $\mathbf{X} \in \mathcal{HT}$  the difference  $\mathbf{X} - \tilde{\Sigma}_{\mathbf{h}}$  is also in  $\mathcal{HT}$  and therefore  $\|\mathbf{X} - \tilde{\Sigma}_{\mathbf{h}} - \Delta\|_{\text{F}}^2 = \|\mathbf{X} - \tilde{\Sigma}_{\mathbf{h}}\|_{\text{F}}^2 + \|\Delta\|_{\text{F}}^2$  where  $\|\Delta\|_{\text{F}}^2$  is constant with respect to  $\mathbf{X}$  and therefore plays no role in the minimization. This proves the equivalence of P1 and P2.  $\blacksquare$

### B. QP estimator

When the dictionary functions  $\psi_i(\xi)$  have overlapping support (e.g., the Gaussian densities in Fig. 4b), the model coefficients  $\{b_i : i = [G]\}$  may take negative values as long as the resulting continuous ASF component is non-negative, i.e.,  $\gamma_c(\xi) = \sum_{i=1}^G b_i \psi_i(\xi) \geq 0, \forall \xi \in [-1, 1]$ . We approximate this infinite-dimensional constraint by defining a sufficiently fine grid of equally spaced points  $\{\xi_1, \dots, \xi_{\tilde{G}}\}$  on  $\xi \in [-1, 1]$  where  $\tilde{G}$  is generally significantly larger than  $G$ , and impose the non-negativity of  $\gamma_c(\cdot)$  at these points. The resulting constraint is

$$\sum_{i=1}^G b_i \psi_i(\xi_j) \geq 0, \quad \forall j \in [\tilde{G}], \quad \iff \quad \tilde{\Psi} \mathbf{b} \geq 0, \quad (22)$$

where the elements of the matrix  $\tilde{\Psi} \in \mathbb{R}^{\tilde{G} \times G}$  are obtained as  $[\tilde{\Psi}]_{i,j} = \psi_j(\xi_i), \forall i \in [\tilde{G}], j \in [G]$ . Then, the estimation problem with dictionary functions with overlapping support is given by

$$\begin{aligned} & \underset{\mathbf{c} \in \mathbb{R}_+^{\tilde{r}}, \mathbf{b} \in \mathbb{R}^G}{\text{minimize}} && \left\| \mathbf{W} \left( \tilde{\mathbf{A}} \mathbf{u} - \tilde{\boldsymbol{\sigma}} \right) \right\|^2, \\ & \text{s.t.} && \tilde{\Psi} \mathbf{b} \geq 0, \end{aligned} \quad (23)$$

where  $\mathbf{u} = [\mathbf{b}^{\text{T}}, \mathbf{c}^{\text{T}}]^{\text{T}}$  is consistently with the definition in (15). Notice that (23) is a QP problem and can be solved using standard QP solvers, such as *quadprog* in MATLAB.

## VI. COEFFICIENTS ESTIMATION BY MAXIMUM-LIKELIHOOD

Instead of directly fitting the Frobenius norm between the sample covariance and the parametric covariance, the model parameters can be estimate by the ML method. Denoting by

$\mathbf{Y} = [\mathbf{y}[1], \dots, \mathbf{y}[N]]$  the matrix of the observed noisy channel samples, the likelihood function of  $\mathbf{Y}$  assuming  $\Sigma_{\mathbf{h}} = \Sigma_{\mathbf{h}}(\mathbf{u})$  in the form of (15) is given by

$$\begin{aligned} p(\mathbf{Y}|\mathbf{u}) &= \prod_{s=1}^N p(\mathbf{y}[s]|\mathbf{u}) \\ &= \prod_{s=1}^N \frac{\exp(-\mathbf{y}[s]^H (\Sigma_{\mathbf{h}}(\mathbf{u}) + N_0\mathbf{I})^{-1} \mathbf{y}[s])}{\pi^M \det(\Sigma_{\mathbf{h}}(\mathbf{u}) + N_0\mathbf{I})} \\ &= \frac{\exp(-\text{tr}((\Sigma_{\mathbf{h}}(\mathbf{u}) + N_0\mathbf{I})^{-1} \mathbf{Y}\mathbf{Y}^H))}{\pi^{MN} (\det(\Sigma_{\mathbf{h}}(\mathbf{u}) + N_0\mathbf{I}))^N}. \end{aligned} \quad (24)$$

Using (24) we can form the minus log-likelihood function  $-\frac{1}{N} \log p(\mathbf{Y}|\mathbf{u})$ . Then, the ML based covariance estimator is obtained by minimizing the minus log-likelihood function with respect to the real and non-negative coefficients vector  $\mathbf{u}$ , which is formulated as the optimization problem:

$$\begin{aligned} \underset{\mathbf{u} \in \mathbb{R}_+^{G+\hat{r}}}{\text{minimize}} \quad & f(\mathbf{u}) = -\frac{1}{N} \log p(\mathbf{Y}|\mathbf{u}) \\ &= \underbrace{\log \det \left( \sum_{i=1}^{G+\hat{r}} u_i \mathbf{S}_i + N_0\mathbf{I} \right)}_{=f_{\text{cav}}(\mathbf{u})} + \underbrace{\text{tr} \left( \left( \sum_{i=1}^{G+\hat{r}} u_i \mathbf{S}_i + N_0\mathbf{I} \right)^{-1} \widehat{\Sigma}_{\mathbf{y}} \right)}_{=f_{\text{vex}}(\mathbf{u})}, \end{aligned} \quad (25)$$

where  $\widehat{\Sigma}_{\mathbf{y}}$  is the sample covariance matrix of the observations defined in (12). Note that the cost function  $f(\mathbf{u})$  in (25) is the sum of a concave and a convex function  $f(\mathbf{u}) = f_{\text{cav}}(\mathbf{u}) + f_{\text{vex}}(\mathbf{u})$  and thus (25) is not a convex problem. It is generally difficult to find the global optimum of a non-convex function such as  $f(\mathbf{u})$ . A standard approach in such cases is to adopt a majorization-minimization (MM) algorithm [37, 38], alternating through two steps with an updating surrogate function that has favorable optimization properties (e.g., convexity) and approximates the lower-bound of the original objective function. Typical examples of MM algorithms are EM method [39], cyclic minimization [40], and the concave-convex procedure [41]. We choose the EM algorithm to iteratively find a good stationary point of  $f(\mathbf{u})$  as we will see that this algorithm yields a computationally efficient update rule and excellent empirical results for the task of estimating the parametric ASF coefficients. Note that although the likelihood function in (25) is in a general form for any family of dictionary functions, the EM method can be applied only in the case where all the matrices  $\mathbf{S}_i$  have rank 1, which is the case when the dictionary functions  $\psi_i(\xi)$  are Dirac delta functions. In contrast, the more general concave-convex procedure (e.g., see [30] for the application in this case) can deal with any type of dictionary, but yields significantly



higher computational complexity, so that it is not suited for large  $M$  (massive MIMO case). In this work, we deal with general dictionary functions using constrained LS, while restrict the use of EM to the case of Diracs dictionary functions.

**Application of the EM algorithm.** With only Dirac delta dictionaries representing for both spikes and continues ASF, we have  $\mathbf{S}_i = \mathbf{a}(\xi_i)\mathbf{a}^H(\xi_i)$ ,  $\forall i \in [G + \hat{r}]$ . Then, the parametric form of channel covariance  $\Sigma_{\mathbf{h}}$  can be reformed as

$$\Sigma_{\mathbf{h}}(\mathbf{u}) = \sum_{i=1}^{G+\hat{r}} u_i \mathbf{S}_i = \mathbf{D}\mathbf{U}\mathbf{D}^H, \quad (26)$$

where  $\mathbf{D} = [\mathbf{a}(\xi_1), \dots, \mathbf{a}(\xi_{G+\hat{r}})]$  and  $\mathbf{U} = \text{diag}(\mathbf{u})$ . Then,  $\Sigma_{\mathbf{y}} = \Sigma_{\mathbf{h}} + N_0\mathbf{I}$  can be formally considered as the covariance matrix of the approximated received samples

$$\mathbf{y}[s] = \sum_{i=1}^{G+\hat{r}} \rho_i[s] \mathbf{a}(\xi_i) + \mathbf{z}[s] = \mathbf{D}\mathbf{x}[s] + \mathbf{z}[s], \quad (27)$$

where  $\mathbf{x}[s] = [\rho_1[s], \dots, \rho_{G+\hat{r}}[s]]^T$  is the latent variable vector containing the instantaneous random path gain, and we have  $\mathbf{x}[s] \sim \mathcal{CN}(\mathbf{0}, \mathbf{U})$ ,  $\forall s \in [N]$  by considering  $\mathbf{u} \in \mathbb{R}_+^{G+\hat{r}}$  as the Gaussian prior variance element-wise corresponding to the Gaussian process  $\mathbf{x}[s]$ .

Under the formulation in (27), the  $N$  noisy samples collected as columns of the matrix  $\mathbf{Y}$  can be written as  $\mathbf{Y} = \mathbf{D}\mathbf{X} + \mathbf{Z}$ , where  $\mathbf{X} = [\mathbf{x}[1], \dots, \mathbf{x}[N]]$  and  $\mathbf{Z} = [\mathbf{z}[1], \dots, \mathbf{z}[N]]$ . The EM algorithm treats  $(\mathbf{Y}, \mathbf{X})$  as the *incomplete data*, where  $\mathbf{X}$  is referred to as *missing data*. Using the fact that  $\mathbf{Y}$  given  $\mathbf{X}$  is Gaussian with mean  $\mathbf{D}\mathbf{X}$  and independent components with variance  $N_0$ , we have that  $p(\mathbf{Y}, \mathbf{X}|\mathbf{u}) = p(\mathbf{Y}|\mathbf{X})p(\mathbf{X}|\mathbf{u})$ , where  $p(\mathbf{Y}|\mathbf{X})$  is a conditional Gaussian distribution that does not depend on  $\mathbf{u}$ . By marginalizing with respect to  $\mathbf{X}$  and taking the logarithm, the log-likelihood function takes on the form of a conditional expectation  $\mathcal{L}(\mathbf{u}) := \log p(\mathbf{Y}|\mathbf{u}) = \log \mathbb{E}_{\mathbf{X}|\mathbf{u}}[p(\mathbf{Y}|\mathbf{X})]$ . The EM algorithm maximizes iteratively the lower bound of  $\mathcal{L}(\mathbf{u})$  by alternating the expectation step (E-step) and the maximization step (M-step) [38] as follows. Let  $\hat{\mathbf{u}}^{(\ell)}$  be the estimate of  $\mathbf{u}$  in the  $\ell$ -th iteration, by introducing a posterior density of  $\mathbf{X}$  as  $p(\mathbf{X}|\mathbf{Y}, \hat{\mathbf{u}}^{(\ell)})$  we have

$$\mathcal{L}(\mathbf{u}) = \log \mathbb{E}_{\mathbf{X}|\mathbf{u}} \left[ \frac{p(\mathbf{Y}|\mathbf{X})p(\mathbf{X}|\mathbf{Y}, \hat{\mathbf{u}}^{(\ell)})}{p(\mathbf{X}|\mathbf{Y}, \hat{\mathbf{u}}^{(\ell)})} \right] = \log \mathbb{E}_{\mathbf{X}|\mathbf{Y}, \hat{\mathbf{u}}^{(\ell)}} \left[ \frac{p(\mathbf{Y}|\mathbf{X})p(\mathbf{X}|\mathbf{u})}{p(\mathbf{X}|\mathbf{Y}, \hat{\mathbf{u}}^{(\ell)})} \right] \quad (28)$$

$$\stackrel{(a)}{\geq} \mathbb{E}_{\mathbf{X}|\mathbf{Y}, \hat{\mathbf{u}}^{(\ell)}} [\log p(\mathbf{Y}|\mathbf{X}) + \log p(\mathbf{X}|\mathbf{u}) - \log p(\mathbf{X}|\mathbf{Y}, \hat{\mathbf{u}}^{(\ell)})] := \tilde{\mathcal{L}}(\mathbf{u}|\hat{\mathbf{u}}^{(\ell)}), \quad (29)$$

where (a) follows Jensen's inequality and the concavity of  $\log(\cdot)$  and gives the lower bound  $\tilde{\mathcal{L}}(\mathbf{u}|\hat{\mathbf{u}}^{(\ell)})$  to the log-likelihood function  $\mathcal{L}(\mathbf{u})$ . The E-step consists of computing  $\tilde{\mathcal{L}}(\mathbf{u}|\hat{\mathbf{u}}^{(\ell)})$ .

Using the joint conditional Gaussianity of  $\mathbf{Y}$  and  $\mathbf{X}$  given  $\mathbf{u} = \hat{\mathbf{u}}^{(\ell)}$ ,  $\tilde{\mathcal{L}}(\mathbf{u}|\hat{\mathbf{u}}^{(\ell)})$  can be evaluated in closed form by computing the conditional mean and covariance of  $\mathbf{x}[s]$  given  $\mathbf{y}[s]$  and  $\hat{\mathbf{u}}^{(\ell)}$ , respectively given by [42]

$$\boldsymbol{\mu}_{\mathbf{x}[s]}^{(\ell)} = \frac{1}{N_0} \boldsymbol{\Sigma}_{\mathbf{x}}^{(\ell)} \mathbf{D}^H \mathbf{y}[s], \quad (30)$$

$$\boldsymbol{\Sigma}_{\mathbf{x}}^{(\ell)} = \left( \frac{1}{N_0} \mathbf{D}^H \mathbf{D} + \left( \hat{\mathbf{U}}^{(\ell)} \right)^{-1} \right)^{-1}, \quad (31)$$

where we define  $\hat{\mathbf{U}}^{(\ell)} = \text{diag}(\hat{\mathbf{u}}^{(\ell)})$ . The M-step consists of computing

$$\hat{\mathbf{u}}^{(\ell+1)} = \arg \max_{\mathbf{u} \in \mathbb{R}_+^{G+\hat{r}}} \tilde{\mathcal{L}}(\mathbf{u}|\hat{\mathbf{u}}^{(\ell)}). \quad (32)$$

Note that  $p(\mathbf{Y}|\mathbf{X})$  and  $p(\mathbf{X}|\mathbf{Y}, \hat{\mathbf{u}}^{(\ell)})$  in (29) do not depend on  $\mathbf{u}$  and thus can be neglected in the M-step. We find the argument of the maximization in the simplified form (details are omitted for brevity)

$$\tilde{\mathcal{L}}(\mathbf{u}|\hat{\mathbf{u}}^{(\ell)}) := \mathbb{E}_{\mathbf{X}|\mathbf{Y}, \hat{\mathbf{u}}^{(\ell)}} [\log p(\mathbf{X}|\mathbf{u})] = \sum_{i=1}^{G+\hat{r}} \left( -N \log(\pi u_i) - \frac{\sum_{s=1}^N \left| \left[ \boldsymbol{\mu}_{\mathbf{x}[s]}^{(\ell)} \right]_i \right|^2 + N \left[ \boldsymbol{\Sigma}_{\mathbf{x}}^{(\ell)} \right]_{i,i}}{u_i} \right). \quad (33)$$

It is observed from (33) that the maximization is decoupled with respect to each component  $u_i$  of  $\mathbf{u}$ . Then, the optimality in the  $\ell$ -th iteration is also easily obtained in closed form. Setting each partial derivative  $\frac{\partial}{\partial u_i} \tilde{\mathcal{L}}(\mathbf{u}|\hat{\mathbf{u}}^{(\ell)})$  for  $i = [G + \hat{r}]$  to zero, we find

$$\hat{u}_i^{(\ell+1)} = \frac{1}{N} \sum_{s=1}^N \left( \left| \left[ \boldsymbol{\mu}_{\mathbf{x}[s]}^{(\ell)} \right]_i \right|^2 + \left[ \boldsymbol{\Sigma}_{\mathbf{x}}^{(\ell)} \right]_{i,i} \right), \quad \forall i \in [G + \hat{r}]. \quad (34)$$

With a initial point  $\hat{\mathbf{u}}^{(0)}$  the ML-EM algorithm iteratively runs the E-step and M-step until the stop condition  $\frac{\|\hat{\mathbf{u}}^{(\ell+1)} - \hat{\mathbf{u}}^{(\ell)}\|}{\|\hat{\mathbf{u}}^{(\ell)}\|} \leq \epsilon_{\text{EM}}$  is met, where  $\epsilon_{\text{EM}}$  is the predefined stop threshold. The initial point can be set as the result of NNLS solution.

## VII. SIMULATION RESULTS

In this section, the proposed constrained LS and ML-EM based estimators are numerically evaluated with the comparison of other benchmarks. This section is organized as follows. First, the benchmarks are introduced. Then, different considered performance metrics are elaborated. Next, the numerical results with only Dirac delta dictionaries are presented and explained. Finally, Dirac delta and Gaussian dictionaries are compared.

### A. Compared benchmarks

In this part, we introduce three benchmarks, with which we compare our proposed algorithms.

#### 1) Toeplitz-PSD Projection

The first benchmark is a intuitively simple approach. We know that the ULA channel covariance is a Toeplitz PSD matrix. Thus, we can project the sample covariance onto the space of Toeplitz-PSD by solving the convex optimization problem:

$$\Sigma_{\mathbf{h}}^{\text{PSD}} = \arg \min_{\Sigma \in \mathcal{HT}} \|\Sigma - \widehat{\Sigma}_{\mathbf{h}}\|_{\text{F}}^2, \quad \text{s.t. } \Sigma \succeq \mathbf{0}. \quad (35)$$

The projected matrix  $\Sigma_{\mathbf{h}}^{\text{PSD}}$  is the covariance estimate. Note that the complexity of this semi-definite programming problem may be high when the number of antennas  $M$  is large.

#### 2) The SPICE Method

The second method we use for comparison is known as sparse iterative covariance-based estimation (SPICE) [25]. This method also exploits the ASF domain but can be only applied with Dirac delta dictionaries. Similar to the parametric covariance model with only Dirac delta dictionaries introduced in (26), assuming Dirac delta dictionaries  $\mathbf{D} = [\mathbf{a}(\xi_1), \dots, \mathbf{a}(\xi_G)]$  of  $G$  array response vectors corresponding to  $G$  AoAs, and defining  $\Sigma = \mathbf{D}\text{diag}(\mathbf{u})\mathbf{D}^{\text{H}}$ , the ASF coefficients  $\mathbf{u}$  is estimated by solving the following convex optimization problem for two cases:

$$\mathbf{u}^* = \begin{cases} \arg \min_{\mathbf{u} \in \mathbb{R}_+^G} \left\| \Sigma^{-1/2} \left( \widehat{\Sigma}_{\mathbf{y}} - \Sigma \right) \right\|_{\text{F}}^2, & N < M, \\ \arg \min_{\mathbf{u} \in \mathbb{R}_+^G} \left\| \Sigma^{-1/2} \left( \widehat{\Sigma}_{\mathbf{y}} - \Sigma \right) \widehat{\Sigma}_{\mathbf{y}}^{-1/2} \right\|_{\text{F}}^2, & N \geq M. \end{cases} \quad (36)$$

The channel covariance estimate is then obtained as  $\Sigma_{\mathbf{h}}^{\text{SPICE}} = \mathbf{D}\text{diag}(\mathbf{u}^*)\mathbf{D}^{\text{H}}$ .

#### 3) Convex Projection Method

This method is proposed in [13] for the ASF estimation by solving a convex feasibility problem  $\widehat{\gamma} = \text{find } \gamma$ , subject to  $\gamma \in \mathcal{S}$ , where

$$\mathcal{S} = \left\{ \gamma : \int_{-1}^1 \gamma(\xi) e^{j\pi m \xi} d\xi = [\widehat{\Sigma}_{\mathbf{h}}]_{m,1}, \quad m = [M], \gamma(\xi) \geq 0, \forall \xi \in [-1, 1] \right\}. \quad (37)$$

This can be solved by applying an iterative projection algorithm, which produces a sequence of functions in  $L_2$  that converges to a function satisfying the constraint  $\gamma \in \mathcal{S}$ . Given the estimated ASF  $\widehat{\gamma}$ , the channel covariance estimation is obtained following (4).

### B. Considered metrics

Denoting a generic covariance estimate as  $\widehat{\Sigma}$ , we use three error metrics to evaluate the estimation quality:

- 1) *Normalized Frobenius-norm Error*: This error is defined as

$$E_{\text{NF}} = \frac{\|\Sigma_{\mathbf{h}} - \widehat{\Sigma}\|_{\text{F}}}{\|\Sigma_{\mathbf{h}}\|_{\text{F}}}. \quad (38)$$

- 2) *Normalized MSE of channel estimation*: Given a noisy channel observation  $\mathbf{y} = \mathbf{h} + \mathbf{z}$ , the optimal estimation of channel vector  $\mathbf{h}$  is obtained via linear MMSE filter  $\widehat{\mathbf{h}} = \widehat{\Sigma} (N_0 \mathbf{I} + \widehat{\Sigma})^{-1} \mathbf{y}$ . Then, this metric considers the normalized mean squared error (MSE) of instantaneous channel estimation:

$$E_{\text{MSE}} = \frac{\mathbb{E}[\|\mathbf{h} - \widehat{\mathbf{h}}\|^2]}{\mathbb{E}[\|\mathbf{h}\|^2]}. \quad (39)$$

Note that the lower bound of this error is obtained using the true channel covariance.

- 3) *Power Efficiency*: This metric evaluates the similarity of dominant subspaces between the estimated and true matrices, which is an important factor in various applications of massive MIMO such as user grouping and group-based beamforming. Specifically, let  $p \in [M]$  denote a subspace dimension parameter and let  $\mathbf{U}_p \in \mathbb{C}^{M \times p}$  and  $\widehat{\mathbf{U}}_p \in \mathbb{C}^{M \times p}$  be the  $p$  dominant eigenvectors of  $\Sigma_{\mathbf{h}}$  and  $\widehat{\Sigma}$  corresponding to their largest  $p$  eigenvalues, respectively. The power efficiency based on  $p$  is defined as

$$E_{\text{PE}}(p) = 1 - \frac{\langle \Sigma_{\mathbf{h}}, \widehat{\mathbf{U}}_p \widehat{\mathbf{U}}_p^{\text{H}} \rangle}{\langle \Sigma_{\mathbf{h}}, \mathbf{U}_p \mathbf{U}_p^{\text{H}} \rangle}. \quad (40)$$

It is noticed that  $E_{\text{PE}}(p) \in [0, 1]$  and the closer it is to 0, the more power is captured by the estimated  $p$ -dominant subspace.

### C. Simulation results

We first provide a performance comparison under only Dirac delta dictionaries with a relatively large number of dictionaries. Then, we provide a comparison under different dictionaries to show the benefit of properly choosing dictionary. In the simulation, we consider a ULA with  $M = 128$  antennas. The SNR is set to 10 dB. The results are averaged over 20 random ASFs and 100 times of random channel realizations for each ASF.

### 1) Comparison under Dirac delta dictionaries

We produce random ASFs in the following general format:

$$\begin{aligned} \gamma(\xi) &= \gamma_d(\xi) + \gamma_c(\xi) \\ &= \frac{\alpha}{r} \sum_{i=1}^r \delta(\xi - \xi_i) + \frac{1-\alpha}{Z} \left( \sum_{k=1}^{n_r} \text{rect}_{\mathcal{A}_k}(\xi) + \sum_{j=1}^{n_g} \text{Gaussian}_{\mathcal{A}_j}(\xi) \right), \end{aligned} \quad (41)$$

where  $r = 2$ ,  $n_r = 2$  and  $n_g = 2$  are set as the number of delta, rectangular and Gaussian functions, respectively.  $Z = \int_{-1}^1 \gamma_c(\xi) d\xi$  is the normalization scalar and  $\alpha = 0.5$  is set to present the power contribution of discrete spikes. Spike locations are chosen uniformly at random over  $[-1, 1]$ , i.e.,  $\xi_i \sim \mathcal{U}([-1, 1])$ . For rectangular functions we have

$$\text{rect}_{\mathcal{A}_k}(\xi) = \begin{cases} 1, & \xi \in \mathcal{A}_k = [\mu_k - \frac{\sigma_k}{2}, \mu_k + \frac{\sigma_k}{2}] \\ 0, & \text{otherwise} \end{cases}, \quad (42)$$

where  $\mu_k$  and  $\sigma_k$  are respectively mean and width of the  $k$ -th rectangular function. For Gaussian functions we have

$$\text{Gaussian}_{\mathcal{A}_j}(\xi) = \begin{cases} \frac{1}{\sigma_j \sqrt{2\pi}} \exp\left(-\frac{(\xi - \mu_j)^2}{2\sigma_j^2}\right), & \xi \in [-1, 1] \\ 0, & \text{otherwise} \end{cases}, \quad (43)$$

where  $\mu_j$  and  $\sigma_j$  are respectively mean and standard deviation of the  $j$ -th Gaussian function. In our simulation, we set  $\mu_1 \sim \mathcal{U}([-1, 0])$ ,  $\mu_2 \sim \mathcal{U}([0, 1])$ ,  $\sigma_k \sim \mathcal{U}([0.1, 0.3])$ ,  $\forall k = 1, 2$  and  $\mu_j \sim \mathcal{U}([-0.7, 0.7])$ ,  $\forall j = 1, 2$ ,  $\sigma_j \sim \mathcal{U}([0.03, 0.04])$ ,  $\forall j = 1, 2$ . The number of dictionaries for continuous part  $\mathcal{G}_c$  is  $G = 2M$ . Note that we only provide  $\mathcal{G}_c$  for SPICE as dictionaries since the process of finding the support of spikes by MUSIC is proposed by us and not included in SPICE algorithm. In Fig. 5, the UL channel covariance estimation error in terms of the normalized Frobenius-norm error, normalized MSE of channel estimation and power efficiency under different sample ratios  $N/M$  are depicted. It is firstly observed that the results of the proposed NNLS and ML methods outperform the results of sample covariance and SPICE for all metrics in all range of sample size. Although the toeplitz-PSD method has very similar Frobenius-norm errors compared to our methods, it performs significantly worse than our methods in terms of channel estimation error. The reason of this can be observed from the results of power efficiency. From Fig. 5c and 5d, we notice that the toeplitz-PSD method estimates the first few significant subspace, e.g.,  $p \leq 20$ , as well as our methods. However, its subspace estimation becomes worse when  $p$  is large, e.g.,  $40 \leq p \leq 50$ .

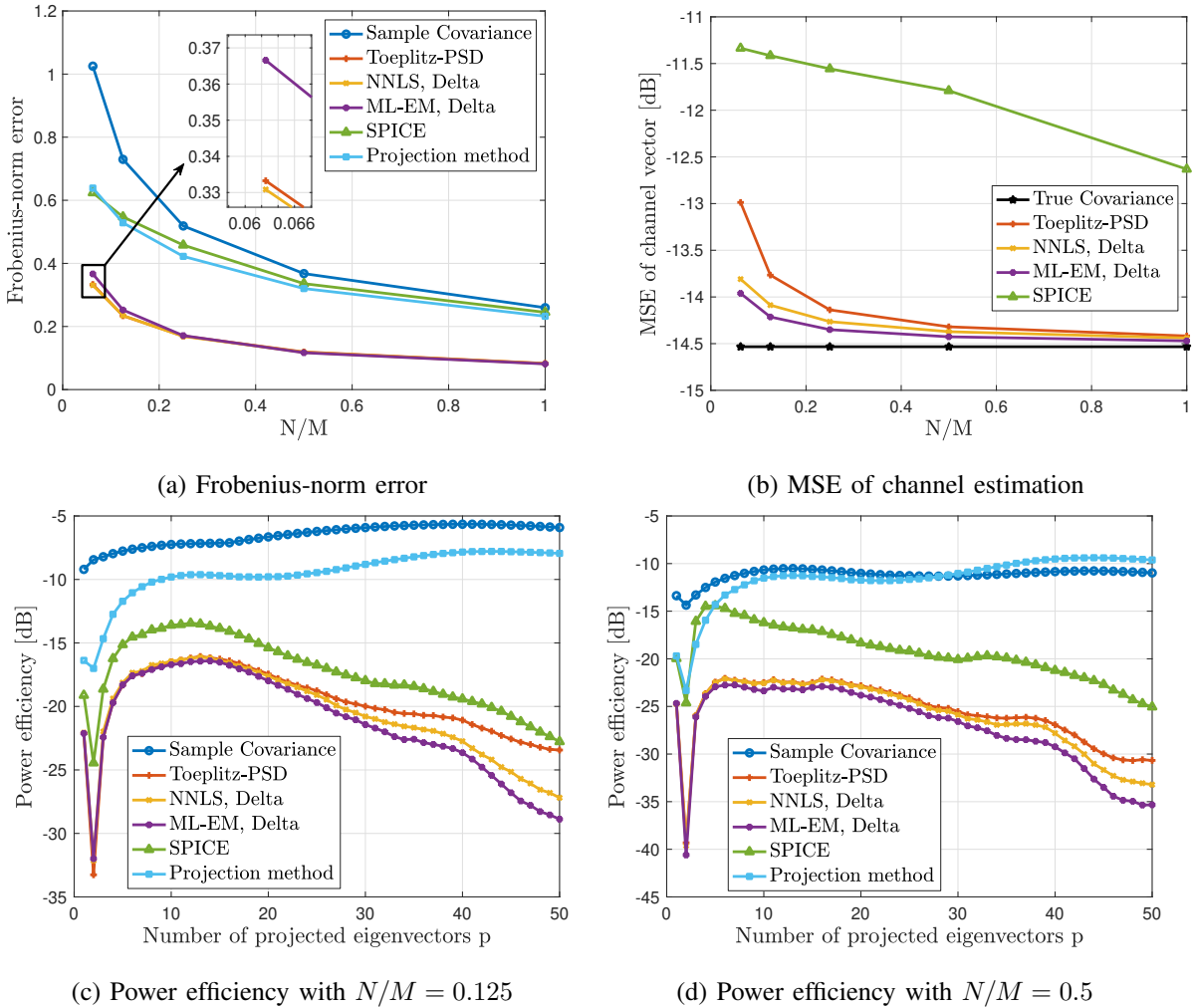


Fig. 5: UL covariance estimation quality comparison.

In Fig. 6, the DL channel covariance estimation error in terms of normalized Frobenius-norm error and power efficiency under sample ratios  $N/M = 0.5$  are depicted. The DL-UL central frequency ratio is set to  $\nu = \frac{f_\nu}{f_0} = 1.1$ . Note that toeplitz-PSD can not provide UL-DL covariance transformation. It is observed that results of SPICE and projection method are much worse compared to the proposed NNLS and ML-EM methods in terms of the Frobenius-norm error and power efficiency. This indicates that our proposed methods can provide a good UL-DL channel covariance transformation.

An example of estimated ASFs in such setting under  $N/M = 1$  is depicted in Fig. 8a. Note that the components of true ASF are separately plotted, and the NNLS results with estimated

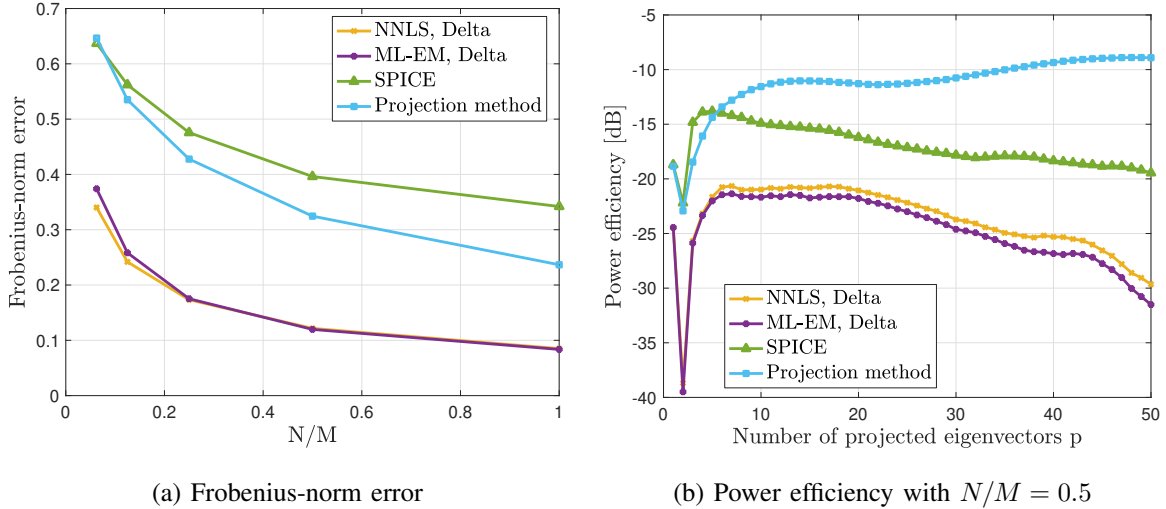


Fig. 6: DL covariance estimation quality comparison with  $\nu = \frac{f_v}{f_0} = 1.1$ .

supports using MUSIC are also separately highlighted. From the local enlarged views, it is clearly observed that the supports of spikes are well estimated via MUSIC. It also shows that the ASF estimation of the proposed NNLS algorithm is much better compared to SPICE method.

## 2) Comparison with Dirac delta and overlapping Gaussian dictionaries

In this part, we show the results based on Dirac delta and Gaussian dictionaries to indicate the importance of finding the proper dictionary. We set a fixed  $N = 32$ . The ASF consists of **no spike** and **3 Gaussian scatterings**, whose means and standard deviation are respectively chosen randomly from  $[-0.7, 0.7]$  and  $[0.03, 0.04]$ . Then, we test the NNLS algorithm with Dirac delta and Gaussian dictionaries as well as the QP estimator with Gaussian dictionaries with  $\tilde{G} = 10000$  under different number of dictionaries. The overlapping Gaussian dictionaries are defined as follows. With the number of dictionaries  $G$ , let  $\tilde{\psi}(\xi)$  be a Gaussian function whose support is limited to  $[0, \frac{2}{G}]$ . The dictionary family  $\{\psi_i(\xi) : i = [G]\}$  consists of shifted versions of  $\tilde{\psi}(\xi)$ , i.e.,  $\psi_i(\xi) = \tilde{\psi}(\xi + 1 - \frac{2i}{G}), i \in [G]$ . The  $\tilde{\psi}(\xi)$  is designed as

$$\tilde{\psi}(\xi) = \begin{cases} \frac{a_0}{\sigma\sqrt{2\pi}} \exp\left(-\frac{(\xi-\mu)^2}{2\sigma^2}\right), & \xi \in [0, \frac{2}{G}] \\ 0, & \text{otherwise} \end{cases}, \quad (44)$$

where  $\mu = \frac{1}{G}$  and  $\sigma = \frac{1}{G\sqrt{2\log(10)}}$  to ensure that the value of the Gaussian function drops to 0.1 of its peak at the boundary points of  $[0, \frac{2}{G}]$ , and  $a_0$  is a normalization scalar such that  $\int_{-1}^1 \tilde{\psi}(\xi) d\xi = 1$ .

The results are shown in Fig. 7. From Fig. 7a and 7b it is observed that the results under Gaussian dictionaries are much better than the results under Dirac delta dictionaries when the number of dictionaries is very less, e.g.,  $G/M \leq 1$ . This is due to the matched model between the chosen Gaussian dictionary and the true ASF. It is also observed that both Frobenius-norm error and channel estimate MSE of NNLS and SPICE under Dirac delta dictionaries decrease dramatically with the increase of the number of dictionaries. Oppositely, the results under Gaussian dictionaries decrease slightly with very small  $G/M$  and become worse when  $G/M > 0.5$ . This is because with the increase of number of dictionaries the overlapping Gaussian dictionary model changes itself from under-parametric to over-parametric. In between, there is a point that the model is fitting with the true ASF and resulted in the best estimate. Additionally, with a very large number of dictionaries the Gaussian dictionaries are more and more similar as Dirac delta dictionaries and thus their results converge to the same value in both Fig. 7a and 7b. The similar behaviour is observed in Fig. 7c and 7d.

We also present two examples of estimated ASFs in such setting under  $G/M = 0.125$  and  $G/M = 2$  in Fig. 8b and Fig. 8c, respectively. It is observed that under  $G/M = 0.125$  the estimated ASF of NNLS with Dirac delta is significantly different from the true ASF due to very small number of dictionaries. Oppositely, the results under Gaussian dictionaries are able to estimate the ASF properly since the dictionaries fit the shape of true diffuse scatterings. On the other hand, under  $G/M = 2$  the overlapping Gaussian dictionaries behave like Dirac delta. In such case all estimated ASFs are similar to each other. This can be also reflected in Fig. 7a, in which the Frobenius-norm error of NNLS-Delta, NNLS-Gaussian and QP-Gaussian converge with the increase of  $G/M$ .

## VIII. CONCLUSION

In this work, we addressed the problem of estimating the covariance matrix of the channel vector from a set of noisy UL pilot observations in massive MIMO systems. By modeling the ASF of the channel as a parametric representation in the angle domain, we proposed the NNLS, QP and ML-EM based estimators to obtain the model parameters. In order to find the discrete scattering components (location of the spikes in the ASF), we adopted MUSIC with a clever clustering of the few large eigenvalues corresponding to the spikes. Theoretical results guarantee that the separation of the spikes with respect to the clutter of eigenvalues due to the diffuse



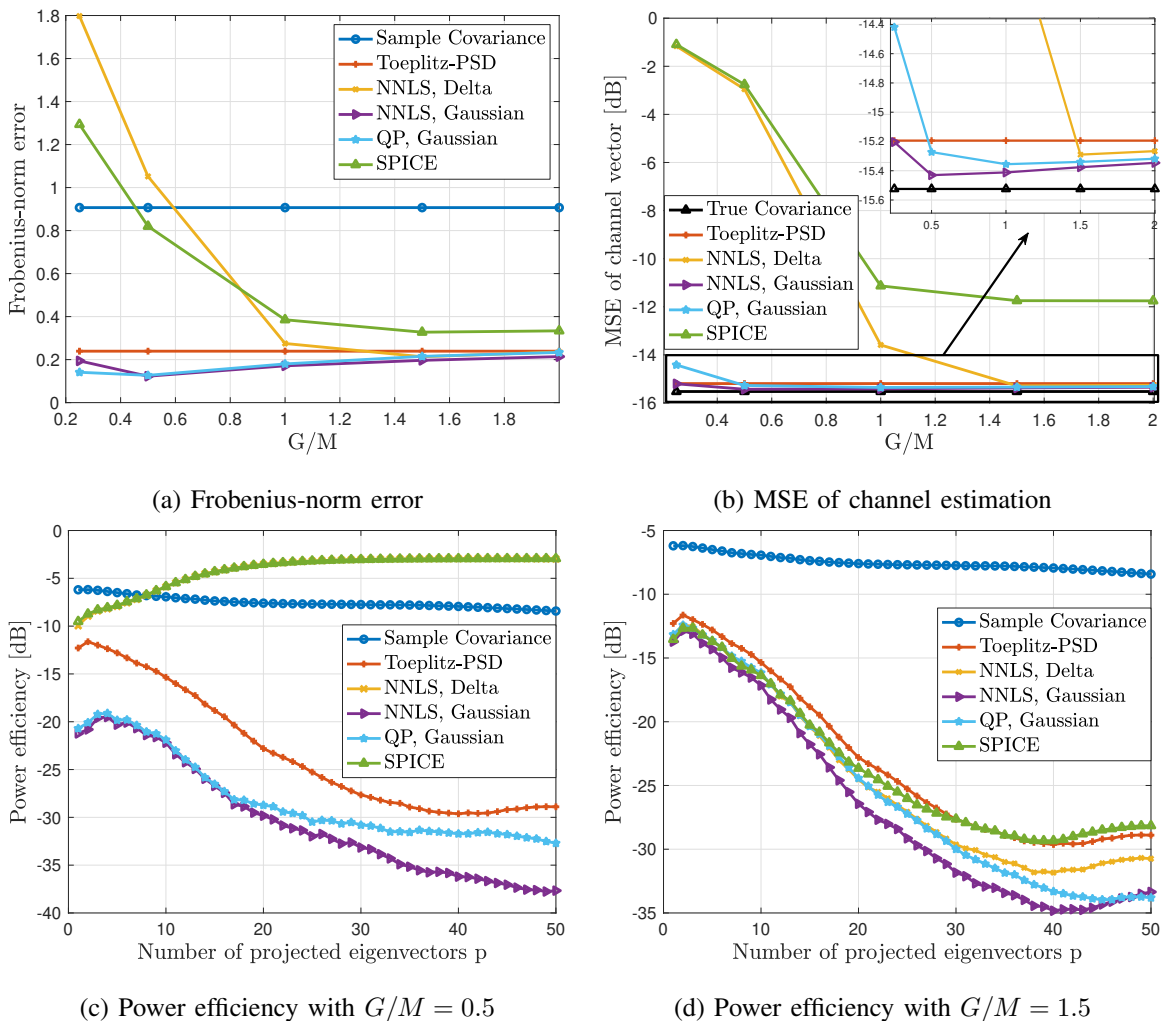


Fig. 7: Comparison with Dirac delta and Gaussian dictionaries in terms of Frobenius-norm error in (a), MSE of channel estimation in (b) and power efficiency in (c), (d) under various  $G/M$ .

scattering components is large, for a large number of antennas. This yields that the spikes support estimation in the massive MIMO regime is very reliable. In addition, our method estimates both the coefficients of the spikes and the coefficients of the diffuse part of the ASF jointly, by one of the methods said above. Extensive numerical simulations show that the proposed methods are superior to several state-of-the-art algorithms in the literature in terms of different performance metrics, especially for a small number of samples, which is particularly relevant for the massive MIMO application.

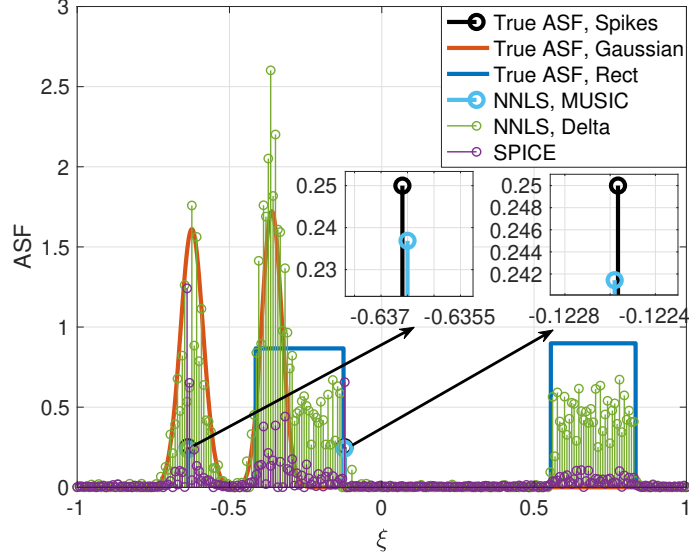
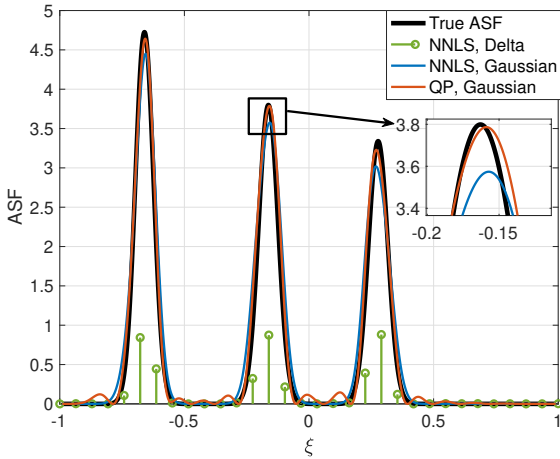
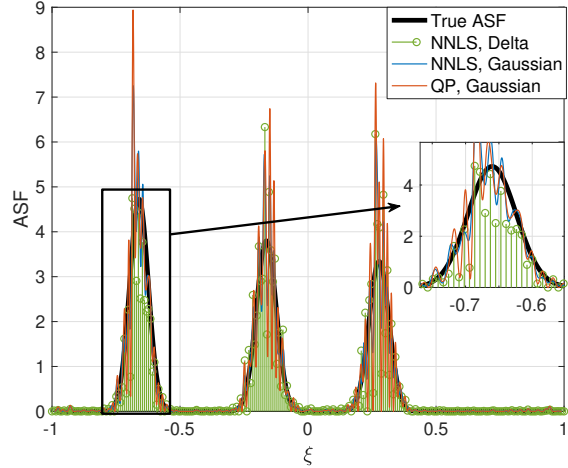
(a) Setting of Sec.VII-C1 under  $N/M = 1$ (b) Setting of Sec.VII-C2 under  $G/M = 0.125$ (c) Setting of Sec.VII-C2 under  $G/M = 2$ 

Fig. 8: Estimated ASF comparison with setting of Sec.VII-C1 under  $N/M = 1$  in (a) and with setting of Sec.VII-C2 under  $G/M = 0.125$  in (b) and  $G/M = 2$  in (c).

## APPENDIX

The Toeplitzed matrix  $\tilde{\Sigma}_{\mathbf{h}}$  is obtained by solving the orthogonal projection problem

$$\tilde{\Sigma}_{\mathbf{h}} = \arg \min_{\Sigma} \|\Sigma - \hat{\Sigma}_{\mathbf{h}}\|_F^2, \quad \text{s.t. } \Sigma \text{ is Hermitian Toeplitz.} \quad (45)$$

Define  $\sigma \in \mathbb{C}^{M \times 1}$  as the first column of  $\Sigma$  and  $\mathcal{P}$  as the operation that projects  $\sigma$  and its conjugate to a Hermitian Toeplitz matrix as  $\Sigma = \mathcal{P}(\sigma)$ . We further define  $\mathcal{K}_i = \{(r, c) : r \leq c \text{ with } [\Sigma]_{r,c} = [\sigma]_i\}$ ,  $i \in [M]$  as the set of all those indices in  $\Sigma$ , in which the  $i$ -th variable  $[\sigma]_i$

appears. Then, the objective function in (45) can be equivalently presented as

$$f(\boldsymbol{\sigma}) = \min_{\boldsymbol{\sigma}} \|\mathcal{P}(\boldsymbol{\sigma}) - \widehat{\boldsymbol{\Sigma}}_{\mathbf{h}}\|_{\text{F}}^2 = \min_{\boldsymbol{\sigma}} \sum_{i=1}^M \sum_{(r,c) \in \mathcal{K}_i} \left| [\boldsymbol{\sigma}]_i - [\widehat{\boldsymbol{\Sigma}}_{\mathbf{h}}]_{r,c} \right|^2. \quad (46)$$

By setting the derivative of  $[\boldsymbol{\sigma}]_i$  to zero, the optimum  $\boldsymbol{\sigma}^*$  is achieved as

$$\frac{\partial f(\boldsymbol{\sigma})}{\partial [\boldsymbol{\sigma}]_i} = \sum_{(r,c) \in \mathcal{K}_i} 2([\boldsymbol{\sigma}]_i - [\widehat{\boldsymbol{\Sigma}}_{\mathbf{h}}]_{r,c}) \stackrel{!}{=} 0, \quad \forall i \in [M], \quad (47)$$

$$\Rightarrow [\boldsymbol{\sigma}^*]_i = \frac{\sum_{(r,c) \in \mathcal{K}_i} [\widehat{\boldsymbol{\Sigma}}_{\mathbf{h}}]_{r,c}}{|\mathcal{K}_i|}, \quad \forall i \in [M], \quad (48)$$

where  $|\mathcal{K}_i|$  denotes the number of elements in  $\mathcal{K}_i$ . Correspondingly,  $\widetilde{\boldsymbol{\Sigma}}_{\mathbf{h}} = \mathcal{P}(\boldsymbol{\sigma}^*)$ .

## REFERENCES

- [1] F. Boccardi, R. W. Heath, A. Lozano, T. L. Marzetta, and P. Popovski, “Five disruptive technology directions for 5G,” *IEEE Communications Magazine*, vol. 52, no. 2, pp. 74–80, 2014.
- [2] T. L. Marzetta, E. G. Larsson, H. Yang, and H. Q. Ngo, *Fundamentals of Massive MIMO*. Cambridge University Press, 2016.
- [3] Z. Chen and C. Yang, “Pilot decontamination in wideband massive MIMO systems by exploiting channel sparsity,” *IEEE Transactions on Wireless Communications*, vol. 15, no. 7, pp. 5087–5100, 2016.
- [4] H. Yin, L. Cottatellucci, D. Gesbert, R. R. Muller, and G. He, “Robust pilot decontamination based on joint angle and power domain discrimination,” *IEEE Transactions on Signal Processing*, vol. 64, no. 11, pp. 2990–3003, 2016.
- [5] S. Haghghatshoar and G. Caire, “Massive MIMO pilot decontamination and channel interpolation via wideband sparse channel estimation,” *IEEE Transactions on Wireless Communications*, vol. 16, no. 12, pp. 8316–8332, 2017.
- [6] M. B. Khalilsarai, S. Haghghatshoar, X. Yi, and G. Caire, “FDD massive MIMO via UL/DL channel covariance extrapolation and active channel sparsification,” *IEEE Transactions on Wireless Communications*, vol. 18, no. 1, pp. 121–135, 2018.
- [7] M. N. Boroujerdi, S. Haghghatshoar, and G. Caire, “Low-complexity statistically robust precoder/detector computation for massive MIMO systems,” *IEEE Transactions on Wireless Communications*, vol. 17, no. 10, pp. 6516–6530, 2018.
- [8] S. Haghghatshoar and G. Caire, “Low-complexity massive MIMO subspace estimation

- and tracking from low-dimensional projections,” *IEEE Transactions on Signal Processing*, vol. 66, no. 7, pp. 1832–1844, 2018.
- [9] ———, “Massive MIMO channel subspace estimation from low-dimensional projections,” *IEEE Trans. on Signal Processing*, vol. 65, no. 2, pp. 303–318, 2017.
- [10] A. Adhikary, J. Nam, J.-Y. Ahn, and G. Caire, “Joint spatial division and multiplexing: the large-scale array regime,” *IEEE Trans. on Inform. Theory*, vol. 59, no. 10, pp. 6441–6463, 2013.
- [11] V. Va, J. Choi, and R. W. Heath, “The impact of beamwidth on temporal channel variation in vehicular channels and its implications,” *IEEE Transactions on Vehicular Technology*, vol. 66, no. 6, pp. 5014–5029, 2016.
- [12] K. Mahler, W. Keusgen, F. Tufvesson, T. Zemen, and G. Caire, “Propagation of multipath components at an urban intersection,” in *2015 IEEE 82nd Vehicular Technology Conference (VTC2015-Fall)*. IEEE, 2015, pp. 1–5.
- [13] L. Miretti, R. L. Cavalcante, and S. Stanczak, “FDD massive MIMO channel spatial covariance conversion using projection methods,” in *2018 IEEE International Conference on Acoustics, Speech and Signal Processing (ICASSP)*. IEEE, 2018, pp. 3609–3613.
- [14] M. B. Khalilsarai, Y. Song, T. Yang, S. Haghghatshoar, and G. Caire, “Uplink-downlink channel covariance transformations and precoding design for FDD massive MIMO,” in *2019 53rd Asilomar Conference on Signals, Systems, and Computers*. IEEE, 2019, pp. 199–206.
- [15] Y. Song, M. B. Khalilsarai, S. Haghghatshoar, and G. Caire, “Deep learning for geometrically-consistent angular power spread function estimation in massive MIMO,” in *GLOBECOM 2020-2020 IEEE Global Communications Conference*. IEEE, 2020, pp. 1–6.
- [16] J. P. González-Coma, P. Suárez-Casal, P. M. Castro, and L. Castedo, “FDD channel estimation via covariance estimation in wideband massive MIMO systems,” *Sensors*, vol. 20, no. 3, p. 930, 2020.
- [17] A. Decurninge, M. Guillaud, and D. T. Slock, “Channel covariance estimation in massive MIMO frequency division duplex systems,” in *Globecom Workshops (GC Wkshps), 2015 IEEE*. IEEE, 2015, pp. 1–6.
- [18] V. A. Marchenko and L. A. Pastur, “Distribution of eigenvalues for some sets of random matrices,” *Matematicheskii Sbornik*, vol. 114, no. 4, pp. 507–536, 1967.

- [19] W. Hachem, P. Loubaton, and J. Najim, “The empirical eigenvalue distribution of a Gram matrix: From independence to stationarity,” *arXiv preprint math/0502535*, 2005.
- [20] R. Couillet and M. Debbah, *Random matrix methods for wireless communications*. Cambridge University Press, 2011.
- [21] M. Pourahmadi, *High-dimensional covariance estimation: with high-dimensional data*. John Wiley & Sons, 2013, vol. 882.
- [22] P. Ravikumar, M. J. Wainwright, G. Raskutti, B. Yu *et al.*, “High-dimensional covariance estimation by minimizing  $\ell_1$ -penalized log-determinant divergence,” *Electronic Journal of Statistics*, vol. 5, pp. 935–980, 2011.
- [23] Y. Chen, A. Wiesel, and A. O. Hero, “Robust shrinkage estimation of high-dimensional covariance matrices,” *IEEE Transactions on Signal Processing*, vol. 59, no. 9, pp. 4097–4107, 2011.
- [24] J. Friedman, T. Hastie, and R. Tibshirani, “Sparse inverse covariance estimation with the graphical lasso,” *Biostatistics*, vol. 9, no. 3, pp. 432–441, 2008.
- [25] P. Stoica, P. Babu, and J. Li, “SPICE: A sparse covariance-based estimation method for array processing,” *IEEE Transactions on Signal Processing*, vol. 59, no. 2, pp. 629–638, 2011.
- [26] S.-F. Chuang, W.-R. Wu, and Y.-T. Liu, “High-resolution AoA estimation for hybrid antenna arrays,” *IEEE Transactions on Antennas and Propagation*, vol. 63, no. 7, pp. 2955–2968, 2015.
- [27] P. Stoica, R. L. Moses *et al.*, *Spectral analysis of signals*. Pearson Prentice Hall Upper Saddle River, NJ, 2005.
- [28] S. Jaeckel, L. Raschkowski, K. Börner, and L. Thiele, “QuaDRiGa: A 3-D multi-cell channel model with time evolution for enabling virtual field trials,” *IEEE Transactions on Antennas and Propagation*, vol. 62, no. 6, pp. 3242–3256, 2014.
- [29] M. J. Wainwright, *High-dimensional statistics: A non-asymptotic viewpoint*. Cambridge University Press, 2019, vol. 48.
- [30] M. B. Khalilsarai, T. Yang, S. Haghghatshoar, and G. Caire, “Structured channel covariance estimation from limited samples in massive MIMO,” in *ICC 2020-2020 IEEE International Conference on Communications (ICC)*. IEEE, 2020, pp. 1–7.
- [31] A. Ali, N. González-Prelcic, and R. W. Heath, “Estimating millimeter wave channels using

- out-of-band measurements,” in *2016 Information Theory and Applications Workshop (ITA)*. IEEE, 2016, pp. 1–6.
- [32] R. O. Schmidt, “Multiple emitter location and signal parameter estimation,” *Antennas and Propagation, IEEE Transactions on*, vol. 34, no. 3, pp. 276–280, 1986.
- [33] P. Stoica and A. Nehorai, “MUSIC, maximum likelihood, and Cramer-Rao bound,” *IEEE Transactions on Acoustics, speech, and signal processing*, vol. 37, no. 5, pp. 720–741, 1989.
- [34] O. Najim, P. Vallet, G. Ferré, and X. Mestre, “On the statistical performance of MUSIC for distributed sources,” in *2016 IEEE Statistical Signal Processing Workshop (SSP)*. IEEE, 2016, pp. 1–5.
- [35] D. Chen and R. J. Plemmons, “Nonnegativity constraints in numerical analysis,” in *The birth of numerical analysis*. World Scientific, 2010, pp. 109–139.
- [36] C. L. Lawson and R. Hanson, “Solving least squares problems prentice-hall,” *Englewood Cliffs, NJ*, 1974.
- [37] D. R. Hunter and K. Lange, “A tutorial on MM algorithms,” *The American Statistician*, vol. 58, no. 1, pp. 30–37, 2004.
- [38] Y. Sun, P. Babu, and D. P. Palomar, “Majorization-minimization algorithms in signal processing, communications, and machine learning,” *IEEE Transactions on Signal Processing*, vol. 65, no. 3, pp. 794–816, 2016.
- [39] A. P. Dempster, N. M. Laird, and D. B. Rubin, “Maximum likelihood from incomplete data via the EM algorithm,” *Journal of the Royal Statistical Society: Series B (Methodological)*, vol. 39, no. 1, pp. 1–22, 1977.
- [40] M. Journée, Y. Nesterov, P. Richtárik, and R. Sepulchre, “Generalized power method for sparse principal component analysis.” *Journal of Machine Learning Research*, vol. 11, no. 2, 2010.
- [41] A. L. Yuille and A. Rangarajan, “The concave-convex procedure (CCCP),” in *Advances in neural information processing systems*, 2002, pp. 1033–1040.
- [42] D. P. Wipf and B. D. Rao, “Sparse Bayesian learning for basis selection,” *IEEE Transactions on Signal processing*, vol. 52, no. 8, pp. 2153–2164, 2004.